

Lattice structure and vibrational properties of the same nano-object

Jannik C. Meyer,^{1,*} Matthieu Paillet,^{2,*} Jean-Louis Sauvajol,² Georg S. Duesberg,³ and Siegmar Roth¹

¹*Max Planck Institute for Solid State Research, Stuttgart, Germany*

²*Groupe de Dynamique des Phases Condensees, Universite de Montpellier II, France*

³*Infineon Technologies Corporate Research, Munich, Germany*

We present a procedure for determining independently the lattice structure and the vibrational properties of the same individual nano-object. For the example of an individual single-walled carbon nanotube we demonstrate the determination of the structural indices (n,m) of the nanotube by electron diffraction and of the frequencies of vibrational modes by micro-Raman spectroscopy. The precise and independent determination of both structure and mode frequencies allows for direct and unambiguous verification of molecular dynamical calculations and of conclusions drawn from Raman-only experiments.

Modeling the dynamics of a physical system at the atomic level requires knowledge, or assumptions, about the lattice structure or the positions of the individual atoms within the object. The properties of nanoscopic objects often depend critically on the position of each atom as finite-size and quantization effects play an important role. For carbon nanotubes, for example, the electronic, mechanical, and vibrational properties vary significantly depending on their structure. Therefore a comparison of experimental data from single objects with theoretical predictions will be directly possible if the structure of the object is known and independently determined.

A carbon nanotube can be considered as a graphene sheet rolled into a cylinder. The nanotube indices (n,m) describe the possible nanotube structures for single-walled nanotubes (SWNTs) [1]. Depending on the indices, the nanotube can be either metallic or semiconducting with varying band-gaps. Also the characteristic features of the Raman spectrum, like the so-called radial breathing mode (RBM), usually in the 100-300 cm⁻¹ frequency range, and the so-called tangential modes (TM), usually within 1500-1600 cm⁻¹, depend on the nanotube indices [2]. As long as modelization is used to derive the structural information from the spectroscopic data, a verification of the model itself is limited. We present an independent determination of the nanotube structure in combination with Raman spectroscopy on the same object.

The structure, that is the indices, can be determined by electron diffraction in a transmission electron microscope (TEM). However combining the electron microscopic investigation with other measurements on the same object is an experimental challenge. A few groups, including our own, have achieved high-resolution transmission electron microscopy and transport measurements on the same individual single-walled carbon nanotube [3, 4]. A combination with electron diffraction has been achieved only for nanotubes with multiple walls [5]. Transport measurements, however, probe not only the properties of the nanotube but also of the contacts, making the interpretation much more difficult.

Raman spectroscopy, on the other hand, directly yields information about the vibrational properties of the investigated

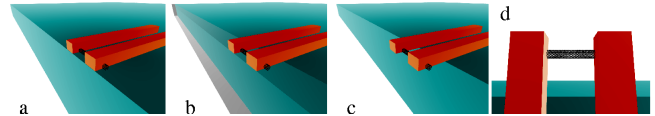


Figure 1: (color online) Schematic illustration of the sample preparation procedure: (a) The substrate is cleaved through a metallic grid which is on top of the carbon nanotubes. (b) The sample is etched in such a way that the structure is mainly undercut from the side, removing the shaded volume. The resulting structure (c) reaches out across the side edge of the substrate. Since the nanotube is still held by the metal contacts and the substrate is no longer in the way, it is accessible for TEM investigations (d, top view).

object. The frequencies of the Raman-active modes of the system can be determined with high accuracy, and can be directly compared with the results of the modelizations of the vibrational dynamics of the investigated nano-object.

We show a simple [but completely new] procedure to create arbitrary nanostructures by electron beam lithography in such a way that access by TEM is possible. The structures, with the carbon nanotubes embedded, are created on the edge of a cleaved substrate and made free-standing with an etching process. Fig. 2 shows two samples with a free-standing section and embedded carbon nanotubes. The free-standing structure can be freely designed by electron beam lithography.

Single-walled carbon nanotubes are grown by chemical vapour deposition (CVD) on highly doped silicon substrates with a 200 nm Silicon dioxide layer [6]. A metal structure consisting of 3 nm Cr and 110 nm Au is created by electron beam lithography on top of the as-grown carbon nanotubes. The substrate is then cleaved through the metal grid structure. An etching process, as illustrated in Fig. 1, is used to obtain freestanding nanotubes: The sample is etched in a 30% KOH bath at 60°C for 7 hours. This removes quickly the bulk Si substrate, and slowly the oxide layer. The etch rate of the doped silicon substrate can be controlled by biasing it with respect to the bath. Since the oxide layer initially acts as a mask, the structure is undercut mainly from the side of the cleaved edge. An undercut of 10 µm can be achieved, and the etching process has to be stopped just when the oxide layer is completely removed. After the etching process, the sample is transferred into deionized water, isopropanol, and acetone before a critical point drying step.

*These authors contributed equally to this work

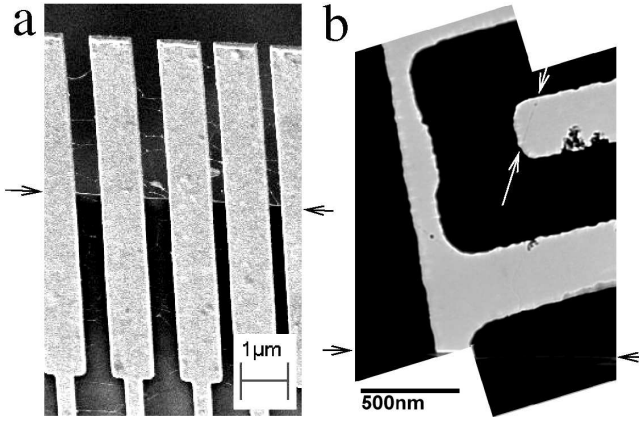


Figure 2: (a) SEM image of a sample showing carbon nanotubes suspended within the metal structure. The dark arrows indicate the edge of the etched substrate: The section above this line is free-standing and accessible by TEM, while the lower part is above the remaining substrate. (b) Low-magnification TEM Overview image of a freestanding metal structure with suspended carbon nanotubes. The nanotube indicated by the white arrow is examined by Raman spectroscopy, high-resolution TEM and electron diffraction. This image is used to locate the carbon nanotube with the optical microscope of the Raman spectrometer.

Since the substrate is no longer in the way, TEM is possible on the free-standing part of the structure on the edge of the substrate. The carbon nanotubes are held in place by the metal structure. Before the micro-Raman experiment, overview TEM images are obtained at low dose and voltage (60 kV) to obtain the position and orientation of the carbon nanotubes with respect to the metal structure (Fig. 2).

Since the metal structure is visible in the optical microscope and the overview images show the position of the nanotubes and their orientation, it is possible to carry out micro-Raman experiments on an oriented single tube. Room-temperature Raman spectra were measured using the Ar/Kr laser lines at 488 nm (2.54 eV), 514.5 nm (2.41 eV) and 647.1 nm (1.92 eV) in the back-scattering geometry on a triple substractive Jobin-Yvon T64000 spectrometer equipped with a liquid nitrogen cooled charge coupled device (CCD) detector. The instrumental resolution is 2 cm^{-1} . A precise positioning of the tubes under the laser spot was monitored with a piezoelectric nano-positioner. In our experimental configuration, the incident light polarization is along the SWNT axis (the Z axis), and no analysis of the polarization of the scattered light is done.

After measuring the Raman spectra, high-resolution TEM images and diffraction images of the Raman-active nanotubes are obtained. We obtain high-resolution images using a Philips CM200 microscope operated at 120 kV, and we record diffraction patterns on image plates in a Zeiss 912Ω microscope operated at 60 kV. It is operated in the Köhler illumination condition with a condenser aperture of $20 \mu\text{m}$. The demagnified image of the condenser aperture illuminates an area of 900 nm in diameter of the sample. We move the nanotube into the illuminated region. Now, only this one nanotube and

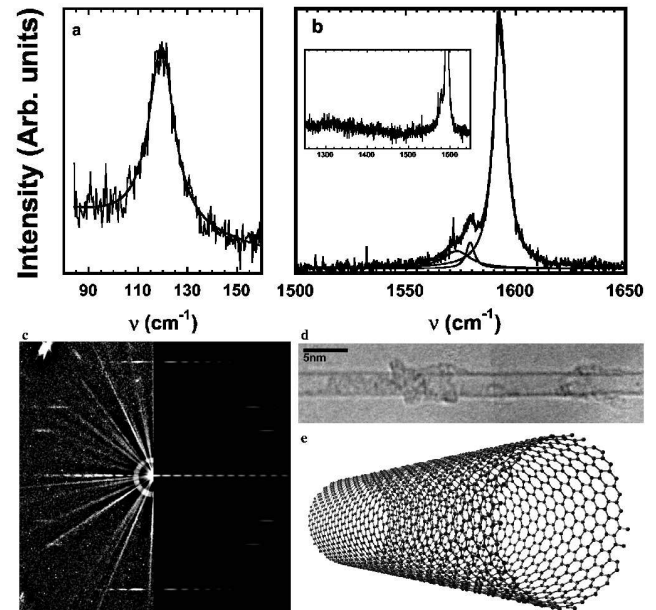


Figure 3: (a) RBM and (b) TM ranges of the Raman spectrum measured on the individual SWNT with a laser energy of 1.92 eV. (c) Diffraction pattern (left), simulated pattern (right) and (d) high-resolution TEM image of the same nanotube. From the diffraction pattern the nanotube can be unambiguously identified as (27,4), while the TEM image confirms the diameter and the presence of only one single nanotube. Image (e) is a structural model of a (27,4) nanotube segment.

a small part of the contact structure is illuminated. To exclude the contact structure from the diffraction pattern, the selected area aperture is used additionally to further limit the effective area to approximately 300 nm in diameter. The energy filter is set to a width 15 eV. The diffraction pattern is exposed onto the image plate for 5 minutes with an illumination angle of 0.1 mrad.

Fig. 3a and b show the Raman spectrum, and Fig. 3c and d show a diffraction pattern and a high-resolution TEM image obtained from the exact same carbon nanotube.

The high-resolution image proves that the investigated tube is indeed individual and not a bundle. From the high-resolution images alone, the nanotube diameter can be estimated only with limited precision. The apparent diameter depends on the defocus value, and the apparent diameter is always smaller than the actual tube diameter [7]. A comparison with image simulations would be possible in principle for a known defocus value, however also the point of zero defocus can not be obtained with the desired precision.

From the diffraction pattern however, it is possible to unambiguously identify the nanotube structure. This nanotube is identified from the diffraction pattern alone as (27,4). By taking into account a C-C distance of $1.42 \pm 0.02 \text{ \AA}$, the diameter of the (27,4) tube is $2.29 \pm 0.03 \text{ nm}$. Its chiral angle is 6.8° . Fig. 3c shows the diffraction pattern and a simulated diffraction pattern of a (27,4) nanotube. We can rule out other indices for which the simulated patterns clearly do not match the measured one, and its diameter of $2.29 \pm 0.03 \text{ nm}$ is con-

sistent with the high-resolution images.

Figures 3a and b show the RBM and TM ranges of the Raman spectrum measured on the SWNT using a 1.92 eV excitation ($\lambda=647.1$ nm), with the polarization in the direction of the tube axis [8]. The (27,4) tube is semiconducting, and with regards to the resonance conditions calculated using a nearest-neighbor tight binding approach [9], its Raman response is expected to be enhanced at 1.7 eV excitation. In agreement with this prediction a detectable signal is only observed for the 1.92 eV excitation in our Raman experiments (available energies were 1.92 eV, 2.41 eV, and 2.54 eV). As expected for the Raman spectrum of an individual SWNT, the spectrum is featured by a single narrow RBM. For the (27,4) tube under investigation, this RBM has a center frequency of 119.5 cm^{-1} (Fig. 3a). In our scattering geometry, a number of lines greater than two in the TM bunch of the Raman spectrum is predicted due to the chiral character of the (27,4) tube [10]. In agreement with this, the profile of the TM bunch, displayed in Fig. 3b, is well fitted by using three main Lorentzian components located at 1593 cm^{-1} , 1579 cm^{-1} and 1573 cm^{-1} . As expected for a semiconducting SWNT, no line broadening as predicted for metallic SWNTs [2] in the TM bunch is observed.

In the inset of figure 3b, the D band range is shown in an expanded scale, and no band is observed in this region. The strength of the D band is expected to be indicative of the amount of defects in the nanotube. The quality of the diffraction pattern indicates a high structural integrity of the nanotube: The structure is periodic, i.e. the indices do not change within the illuminated region and the amount of defects is low. The high-resolution TEM image provides an upper limit for the „endfloats“*amount of amorphous carbon on the tube, since additional carbon is clearly deposited during the TEM analysis. This is in agreement with the interpretation of the D-band as an indicator of defects and amorphous carbon coating. The nanotubes in our samples are completely free-standing, separated and sufficiently clean; most environmental influences on the nanotube spectra can be excluded.

A huge number of experiments and modelization efforts

were made to relate the radial breathing mode (RBM) frequency to the nanotube structure. A review and summary of various models and experiments is given in [11]. Our experimental approach gives access to a first accurate and independent determination of a specific SWNT diameter, at the same time with its RBM frequency. For a free-standing individual SWNT, the RBM frequency ν is expected to be inversely proportional to the nanotube diameter d , i.e. $d = A/\nu$ [11]. From the results obtained on the (27,4) SWNT, a proportionality constant of $A=273\pm10\text{ nm.cm}^{-1}$ is found. This surprisingly high value either indicates that the models are underestimating the RBM frequency (see table 8.2 in Ref.[11]), or that this simple RBM vs. diameter relationship can not be extrapolated up to the relatively large diameter of this tube. However for a precise estimation of the RBM vs. tube diameter relationship, a diffraction analysis of many tubes with a wide distribution of diameters is required.

As a conclusion, we have obtained Raman spectra for a precisely known structure, determined by electron diffraction and high-resolution TEM imaging. A measurement of the vibrational modes for a precisely known structure provides the ultimate test for molecular-dynamics simulations. Both the micro-Raman spectroscopy and the electron microscopic investigation are done on a freely suspended object without an influence from an environment, substrate or contact. We expect that this procedure, due to the freely designable free-standing structure, can be adopted to various nano-objects or macromolecules to combine electron microscopic structural analysis with Raman spectroscopy and potentially other investigations (transport, AFM) on the same object. Also, the possibility to create arbitrary free-standing structures may facilitate novel in-situ experiments in the TEM.

The authors acknowledge financial support by the EU project CARDECOM and the BMBF project INKONAMI. We thank xlith.com for lithography services. We thank P. Poncharal, A. Zahab, C. Koch, K. Hahn, M. Kelsch, F. Phillip and M. Rühle for support and helpful discussions.

This article has been submitted to Applied Physics Letters (<http://apl.aip.org>)

[1] S. Iijima and T. Ichihashi, *Nature* **363**, 603 (1993).
 [2] M. S. Dresselhaus and P. C. Eklund, *Advances in Physics* **49**, 705 (2000).
 [3] J. C. Meyer, D. Obergfell, S. Yang, S. Yang, and S. Roth, *Appl. Phys. Lett.* **85**, 2911 (2004).
 [4] A. Y. Kasumov, R. Deblock, M. Kociak, B. Reulet, H. Bouchiat, I. I. Khodos, Y. B. Gorbatov, V. T. Volkov, C. Journet, and M. Burghard, *Science* **284**, 1508 (1999).
 [5] M. Kociak, K. Suenaga, K. Hirahara, Y. Saito, T. Nakahira, and S. Iijima, *Phys. Rev. Lett.* **89**, 155501 (2002).
 [6] M. Paillet, V. Jourdain, P. Poncharal, J.-L. Sauvajol, A. Zahab, J. C. Meyer, S. Roth, N. Cordente, C. Amiens, and B. Chaudret, *J. Phys. Chem. B* **108**, 17112 (2004).
 [7] C. Quin and L.-M. Peng, *Phys. Rev. B* **65**, 155431 (2002).
 [8] G. S. Duesberg, I. Loa, M. Burghard, K. Syassen, and S. Roth, *Phys. Rev. Lett.* **85**, 5436 (2000).
 [9] H. Kataura, Y. Kumazawa, Y. Maniwa, S. Suzuki, Y. Ohtsuka, and Y. Achiba, *Synth. Met.* **103**, 2555 (1999).
 [10] A. Jorio, M. A. Pimenta, A. G. Souza-Filho, G. G. Samsonidze, M. S. Unlu, B. B. Goldberg, R. Saito, G. Dresselhaus, and M. S. Dresselhaus, *Phys. Rev. Lett.* **90**, 107403 (2003).
 [11] S. Reich, C. Thomsen, and J. Maultzsch, *Carbon nanotubes. basic concepts and physical properties* (Wiley-VCH, 2004).